

# HMX POLYMORPHISM: VIRTUAL MELTING GROWTH MECHANISM, CLUSTER-TO-CLUSTER NUCLEATION MECHANISM AND PHYSICALLY BASED KINETICS

Valery I. Levitas,<sup>1</sup> Laura B. Smilowitz,<sup>2</sup> Bryan F. Henson,<sup>2</sup> and Blaine W. Asay<sup>2</sup>

<sup>1</sup>*Iowa State University, Departments of Mechanical Engineering, Aerospace Engineering, and Material Science and Engineering, Ames, Iowa 50011, USA*

<sup>2</sup>*Los Alamos National Laboratory, Los Alamos, NM 87545, USA*

## ABSTRACT

A fully physically-based thermodynamic and kinetic model of the  $\beta \leftrightarrow \delta$  phase transformation in energetic crystal HMX crystal embedded in polymeric binder is developed. It is based on a new nucleation mechanism via melt mediated nano-cluster transformation and the recently formulated growth mechanism via internal stress-induced virtual melting. During the nucleation, nano-sized clusters of  $\beta$  phase dissolve in a molten binder and transform diffusively into  $\delta$  phase clusters. During the interface propagation, internal stresses induced by transformation strain cause the melting of the stressed  $\delta$  phase much below (120K) the melting temperature and its immediate resolidification into the unstressed  $\delta$  phase. These mechanisms explain numerous puzzles of HMX polymorphism and result in local and overall transformation kinetics that are in good agreement with experiments.

## NOMENCLATURE

B	Bulk modulus of the HMX
$c$	Volume fraction of the $\delta$ phase
$c_0$	Volume fraction of operational nucleus
$h_r$	Heating rate
$E_n$	Activation energy for nucleation
$g^e$	Elastic energy of the internal stresses
$h$	Planck's constant
$k$	Boltzmann's constant
$K$	Bulk modulus of the liquid
$M$	HMX molecular weight
$p$	Pressure

$r_c$	Radius of the critical cluster
$R$	Gas constant
$t_n$	Nucleation time
$t_0$	Time of appearance of operational nucleus
$\bar{t}_0$	Pre-exponential factor
$t_{0.5}$	Time to half conversion
$t_f$	Time to reach the volume fraction $f$
$v$	Velocity of the $\beta - \delta$ phase interface
$v_{av}$	Averaged interface velocity over the total $\beta - \delta$ interface area $\Sigma$
$\bar{v}_0$	Pre-exponential factor
$V$	Volume of the crystal
$V_n$	Volume of the $\delta$ phase nucleus
$V_l$	Volume of liquid
$\gamma$	Interface energy
$\Delta h_{\beta \rightarrow \delta}$	Change in the molar enthalpy during the $\beta \rightarrow \delta$ phase transformation
$\Delta g_{\beta \rightarrow \delta}$	Change in the molar Gibbs potential during the $\beta \rightarrow \delta$ transformation
$\Delta G_{\beta \rightarrow \delta}$	Change in the Gibbs potential per unit volume during the $\beta \rightarrow \delta$ phase transformation
$\Delta s_{\beta \rightarrow \delta}$	Change in the molar entropy during the $\beta \rightarrow \delta$ phase transformation
$\Delta v_{\beta \rightarrow \delta}$	Change in the molar volume during the $\beta \rightarrow \delta$ phase transformation
$\Delta \gamma$	Change in surface energy
$\varepsilon^t$	Volumetric transformation strain for $\beta \rightarrow \delta$ phase transformation
$\varepsilon^c$	Volumetric strain due to cracking
$\varepsilon_{\delta-m}^t$	Volumetric transformation strain for solidification
$\varepsilon^\theta$	Volumetric thermal expansion strain
$\varepsilon_0$	Volumetric strain in the liquid
$\theta$	Temperature
$\theta_e$	Phase equilibrium temperature between $\beta$ and $\delta$ phases
$\theta_m$	Melting temperature
$\theta_i$	Temperature at which phase transformation criterion is met
$\theta_0$	Nucleation temperature
$\rho$	Mass density

## INTRODUCTION

PBX 9501 is an important high explosive with wide applications that is currently under intensive study in governmental laboratories and academia. The PBX 9501 formulation consists of 94.9% by weight of the organic energetic crystals HMX (octahydro-1,3,5,7-tetranitro-1,3,5,7-tetrazocine) with the remainder being a polymeric binder. HMX is subjected to the reconstructive  $\beta \rightarrow \delta$  phase transformation (PT) above 432K. This PT is accompanied by large volume expansion which produces huge internal stresses within HMX that affect the transformation thermodynamics, kinetics, and microstructure. Such a volume change also creates internal stresses within the PBX formulation as

well as within a macroscopic sample if its deformation is restricted (for example, by rigid walls). Knowledge of the kinetics of the  $\beta \leftrightarrow \delta$  PT equation is very important not only because of these stresses but also because of the greater sensitivity<sup>1</sup> and different properties of the  $\delta$  phase.

Pioneering experiments on the  $\beta \leftrightarrow \delta$  PT have been reported in various papers.<sup>2-6</sup> There are a number of phenomenological kinetic models for the  $\beta \leftrightarrow \delta$  PT<sup>7-10</sup> which agree well with experiments in some temperature range at ambient pressure. The main drawback of any phenomenological model is the impossibility to apply it beyond the region of parameters (temperature and pressure evolution) where it is directly confirmed experimentally. In most cases, these data are generated under zero pressure.<sup>7-10</sup> Analysis of these models can be found in Levitas et al.<sup>11</sup> In two particular cases of experiments under high pressure,<sup>4,12</sup> the results are not well understood. In one experiment at high temperatures,<sup>4</sup> the experimental slope of the pressure – temperature transformation line cannot be described using known thermodynamically calculated  $\beta - \delta$  equilibrium line, probably due to chemical decomposition. In another,<sup>12</sup> the beta-delta phase transition is observed at temperatures well below the equilibrium temperature subsequent to release of a pressurized sample. We cannot currently incorporate these data in our model. High pressure experiments in<sup>13</sup> were performed at room temperature and not related to  $\beta - \delta$  PT.

In contrast, the extension of physical mechanism-based models beyond the range of parameters where they are checked experimentally is much more reliable. Along this direction, we suggested recently<sup>11,14,15</sup> that the  $\beta \leftrightarrow \delta$  PT in the HMX energetic crystal occurs via the virtual melting mechanism. The large energy of elastic stresses, induced by transformation strain (that transforms a unit cell of the parent phase into a unit cell of the product), increases the driving force for melting and reduces the melting temperature by approximately 120°K. Immediately after melting, elastic stresses relax and the unstable melt solidifies into the stable product phase. Fast solidification in a thin layer leads to nanoscale cracking which does not, however, affect the thermodynamics and kinetics of the  $\beta \leftrightarrow \delta$  PT. Thus, virtual melting represents a new mechanism of solid-solid PT, stress relaxation and loss of coherence at a moving solid-solid interface. Our theoretical predictions are qualitatively and quantitatively confirmed by sixteen experimental observations of an HMX system.<sup>11,14,15</sup> The virtual melting mechanism has been incorporated into several kinetic models by combination with several phenomenological nucleation models.<sup>11,14,16</sup> We, however, found<sup>17-18</sup> that even the most advanced kinetic model using a phenomenological nucleation kinetics<sup>11,16</sup> exhibits contradictory results when applied to either the high pressure regime or cyclic PT.

In the current paper, we review and further developed a new physical nucleation mechanism in HMX imbedded in polymeric binder via melt mediated nano-cluster transformation.<sup>17-19</sup> It allows us to explain extremely unusual nucleation occurring very close ( $0.6^\circ\text{K}$ ) to the phase equilibrium temperature  $\theta_e$ . A combination of nucleation kinetics based on this mechanism and the growth kinetics based on virtual melting results in a fully physical model for the overall transformation kinetics.

The main limitations of the model are as follows: a) Nucleation model requires presence of the nitroplasticizer. For other binder material (e.g., estane<sup>20</sup>), nano-cluster transformation mechanism may work but requires new calibration of parameters. Without binder, nucleation occurs at the specific nucleating defects which may be inclusions of the solvent used in HMX synthesis<sup>20</sup> or some stress concentrators. b) Material heterogeneity and consequently statistical distribution of material parameters is neglected. c) Effect of impurities is neglected as well.

The paper is organized in the following way. In Section II, the main thermodynamic functions for the  $\beta \rightarrow \delta$  PT and melting of the  $\beta$  and  $\delta$  phases are presented. They are used in subsequent sections to develop a physically based nucleation and growth kinetics for the  $\beta \rightarrow \delta$  PT. In Section III, a new nucleation mechanism for reconstructive solid-solid PT in HMX via melt mediated nano-cluster transformation is described. Our preliminary observations<sup>20</sup> led us to a hypothesis that  $\beta$  HMX dissolves in the liquid medium (in nitroplasticizer), and at temperatures above  $\theta_e$  nucleates the  $\delta$  phase at the interface between the HMX and the liquid. As we will show below, such a mechanism does completely remove the energy of elastic stresses. However, here we find that because of high interface energy such a homogeneous or heterogeneous nucleation is kinetically impossible close to the phase equilibrium temperature.

In this paper, we suggest that the *liquid medium contains nanometer size clusters of  $\beta$  phase*, which may appear while HMX is being dissolved in the liquid by dissolution and destruction of HMX crystalline surface asperities. If such a cluster undergoes the  $\beta \rightarrow \delta$  PT, the change in interface energy can be small enough (or even negative) to allow nucleation near the phase equilibrium temperature. The kinetic equation for nucleation is derived. We first reported on this mechanism in a short letter.<sup>19</sup>

In Section IV, the kinetic equations for the  $\beta - \delta$  interface velocity and volume fraction of the  $\delta$  phase due to growth are derived based on the virtual melting growth mechanism.<sup>11,14,15</sup> In Section V, both nucleation and growth kinetics are combined to model the overall kinetics of the  $\beta - \delta$  PT. The temperature dependence of both interface propagation velocity and volume fraction of the  $\delta$

phase is in good agreement with various experiments under isothermal conditions and zero pressure. Section VI contains the concluding remarks.

### THERMODYNAMICS OF $\beta - \delta$ PHASE TRANSFORMATION AND MELTING IN HMX

Along the lines described in various papers,<sup>11,14,16</sup> we determine the thermodynamic functions necessary for the development of our kinetic models. The molar thermodynamic driving force for the  $\beta \rightarrow \delta$  PT is

$$-\Delta g_{\beta \rightarrow \delta} = -(\Delta h_{\beta \rightarrow \delta} - \theta \Delta s_{\beta \rightarrow \delta}) - p \Delta v_{\beta \rightarrow \delta}, \quad (1)$$

where  $\Delta g_{\beta \rightarrow \delta}$ ,  $\Delta h_{\beta \rightarrow \delta}$ ,  $\Delta s_{\beta \rightarrow \delta}$ , and  $\Delta v_{\beta \rightarrow \delta}$  are the change in the molar Gibbs potential, enthalpy, entropy, and volume during the  $\beta \rightarrow \delta$  PT;  $\theta$  is the temperature and  $p$  is the pressure. Since the maximum pressure at which the  $\beta \rightarrow \delta$  PT is possible is less than 0.245 GPa (pressure at the triple point),<sup>16</sup> and the bulk modulus is  $B = 15$  GPa,<sup>21</sup> the pressure dependence of the bulk moduli in such pressure range can be neglected. The change in elastic energy is then defined as  $0.5p^2 (1/B_\beta - 1/B_\delta)$ . Since literature values of the bulk moduli of HMX differ significantly,<sup>21-22</sup> and since the difference between  $B_\delta$  and  $B_\beta$  should be relatively small, the change in elastic energy is neglected in Eq. (1). We note that there is some scatter in the thermodynamic data. However, assuming constant transformation enthalpy  $\Delta h_{\beta \rightarrow \delta} = 9.8 \text{ kJ/mol}$ ,<sup>7-8</sup> and the entropy related to enthalpy through phase equilibrium temperature  $\theta_e = 432 \text{ K}$  (within a specific range<sup>2,3</sup>), i.e.  $\Delta s_{\beta \rightarrow \delta} = \Delta h_{\beta \rightarrow \delta} / \theta_e = 22.68 \text{ J/molK}$ , we obtain

$$-\Delta g_{\beta \rightarrow \delta} = \Delta s_{\beta \rightarrow \delta} (\theta - \theta_e) - p \Delta v_{\beta \rightarrow \delta}, \quad (2)$$

Note that the phase equilibrium temperature may depend on impurities (in particular, RDX). We choose  $\theta_e = 432 \text{ K}$  since it provides the best fit for the various interface velocity experiments.<sup>11,15,16</sup> Since volumetric transformation strain  $\epsilon^t = \frac{\rho_\beta}{\rho_\delta} - 1$ , then

$$\Delta v_{\beta \rightarrow \delta} = M \left( \frac{1}{\rho_\delta} - \frac{1}{\rho_\beta} \right) = \frac{M}{\rho_\beta} \left( \frac{\rho_\beta}{\rho_\delta} - 1 \right) = M \frac{\epsilon^t}{\rho_\beta}, \quad (3)$$

where  $M \simeq 0.296 \text{ kg/mol}$  is the HMX molecular weight and  $\epsilon^t = 0.08$ ,<sup>21</sup> the mass density of the  $\beta$  phase at phase equilibrium temperature  $\theta = 432^\circ \text{ K}$  is estimated by equation  $\rho_\beta = 1905 / (1 + \epsilon_\beta^\theta) = 1873 \text{ kg/m}^3$ , where the mass density at  $300^\circ \text{ K}$  is  $1905 \text{ kg/m}^3$  (from Weese and Burnham<sup>23</sup>), and  $\epsilon_\beta^\theta$  is determined in Herrmann, et al.<sup>24</sup> The mass density of the  $\delta$  phase at  $\theta = 432^\circ \text{ K}$  is  $\rho_\beta = \rho_\beta / (1 + \epsilon_0^t) = 1734 \text{ kg/m}^3$ . Then  $\Delta v_{\beta \rightarrow \delta} = 1.264 \cdot 10^{-5} \text{ m}^3/\text{mol}$  (in Henson et al.,<sup>7</sup>  $\Delta v_{\beta \rightarrow \delta} = 1.14 \cdot 10^{-5} \text{ m}^3/\text{mol}$  is used which corresponds to  $\epsilon^t = 0.07$ ). The thermodynamic

driving force for the  $\beta \rightarrow \delta$  PT per unit volume which we will need in the nucleation problem is

$$-\Delta G_{\beta \rightarrow \delta} = -\Delta g_{\beta \rightarrow \delta} \rho / M = (\Delta s_{\beta \rightarrow \delta} (\theta - \theta_e) - p \Delta v_{\beta \rightarrow \delta}) \rho / M \quad (4)$$

Similarly, the molar thermodynamic driving force for melting of  $\beta$  and  $\delta$  phases are

$$-\Delta g_{\beta \rightarrow m} = \Delta s_{\beta \rightarrow m} (\theta - \theta_{m,\beta}) - p \Delta v_{\beta \rightarrow m} \quad (5)$$

and

$$-\Delta g_{\delta \rightarrow m} = \Delta s_{\delta \rightarrow m} (\theta - \theta_{m,\delta}) - p \Delta v_{\delta \rightarrow m} \quad (6)$$

Here,  $\theta_{m,\beta}$  and  $\theta_{m,\delta}$  are the melting temperatures of the  $\beta$  and  $\delta$  phases at ambient pressure, respectively. The melting temperature of the  $\delta$  phase reduces with HMX decomposition and that is why it should depend on the heating rate. We choose  $\theta_{m,\delta} = 550^\circ\text{K}$  which is within the range given in Cady and Smith<sup>2</sup> and Teetsov and McCrone.<sup>3</sup> (Note that in Levitas et al.<sup>11,14,15</sup> we used  $\theta_{m,\delta} = 551^\circ\text{K}$ ). Taking the enthalpy of melting of the  $\delta$  phase as  $\Delta h_{\delta \rightarrow m} = 69.9 \text{ kJ}/(\text{mole K})$ <sup>7, 8</sup> we obtain the entropy of melting of the  $\delta$  phase  $\Delta s_{\delta \rightarrow m} = \Delta h_{\delta \rightarrow m} / \theta_{m,\delta} = 127.09 \text{ J}/(\text{mole K})$ . From the temperature independent enthalpy and entropy of these transformations, we obtain the enthalpy and entropy of melting of the  $\beta$  phase:  $\Delta h_{\beta \rightarrow m} = \Delta h_{\beta \rightarrow \delta} + \Delta h_{\delta \rightarrow m} = 79.7 \text{ kJ}/\text{mole}$  and  $\Delta s_{\beta \rightarrow m} = \Delta s_{\beta \rightarrow m} + \Delta s_{\delta \rightarrow m} = 149.77 \text{ J}/(\text{mole K})$ . The melting temperatures of the  $\beta$  phase is then  $\theta_{m,\beta} = \Delta h_{\beta \rightarrow m} / \Delta s_{\beta \rightarrow m} = 532^\circ\text{K}$ . This is higher than  $518.5^\circ\text{K}$  given in Teetsov and McCrone<sup>3</sup> and Cady,<sup>6</sup> but is close to our estimate  $531.3^\circ\text{K}$  (see Levitas et al.,<sup>11</sup> Section 4i) based on the extrapolation of the thermodynamic data from Herrmann et al.<sup>25</sup> This difference may be related to the inaccuracy of interpolation of data because of a possible temperature dependence of the transformation enthalpy and entropy; however, it is not important for the current study of the  $\beta - \delta$  PT. The change in molar volume during melting of the  $\beta$  and  $\delta$  phases are:  $\Delta v_{\beta \rightarrow m} = 2.330 \cdot 10^{-5} \text{ m}^3/\text{mole}$  ( $\epsilon'_{\beta \rightarrow m} = 0.147$ ) and  $\Delta v_{\delta \rightarrow m} = \Delta v_{\beta \rightarrow m} - \Delta v_{\beta \rightarrow \delta} = 1.066 \cdot 10^{-5} \text{ m}^3/\text{mole}$  ( $\epsilon'_{\delta \rightarrow m} = 0.067$ ) (from Henson et al.<sup>7</sup> and Smilowitz et al.<sup>8</sup> Since in Henson et al.<sup>7</sup> we used  $\Delta v_{\beta \rightarrow \delta} = 1.14 \cdot 10^{-5} \text{ m}^3/\text{mole}$ ,  $\Delta v_{\delta \rightarrow m} = 1.19 \cdot 10^{-5} \text{ m}^3/\text{mole}$  was obtained in that work.

Note that the only independent parameters important for the current study of the  $\beta - \delta$  PT are  $\Delta h_{\beta \rightarrow \delta} = 9.8 \text{ kJ}/\text{mol}$ ,  $\theta_e = 432^\circ\text{K}$ ,  $\Delta h_{\delta \rightarrow m} = 69.9 \text{ kJ}/(\text{mole K})$ ,  $\Delta v_{\beta \rightarrow \delta} = 1.264 \cdot 10^{-5} \text{ m}^3/\text{mol}$  and  $\Delta v_{\delta \rightarrow m} = 1.066 \cdot 10^{-5} \text{ m}^3/\text{mole}$ , since only they participate in the kinetic equation for the  $\beta - \delta$  PT [see Eqs. (16), (19) and (20)]. That is why the uncertainty in other parameters above does not affect our results. The phase equilibrium lines for  $\beta - \delta$  PT and melting of  $\beta$  and  $\delta$  phases are obtained by setting the driving force to zero. This can be described by the equations:

$$p_{\beta \rightarrow \delta}(\text{MPa}) = -775.139 + 1.794\theta ; \quad (7)$$

$$p_{\beta-m}(MPa) = -3420.600 + 6.428\theta ; \quad (8)$$

$$p_{\delta-m}(MPa) = -6557.22 + 11.922\theta . \quad (9)$$

The pressure-temperature phase equilibrium diagram based on Eqs. (7)–(9) is presented in Fig. 1. The key point is that with growing pressure the difference in temperature between the  $\beta$ – $\delta$  equilibrium and melting of  $\beta$  and  $\delta$  phase's lines reduces. This makes the *virtual melting PT mechanism even more probable at high pressure than at ambient pressure*. The triple point corresponds to  $\theta = 570.224^\circ\text{K}$  and  $p = 0.245\text{GPa}$ . The difficulties to experimentally access the high temperature part of the phase diagram are related to decomposition of HMX. This may explain discrepancy between thermodynamic Eqs. (7)–(9) and experiments in<sup>4</sup>.

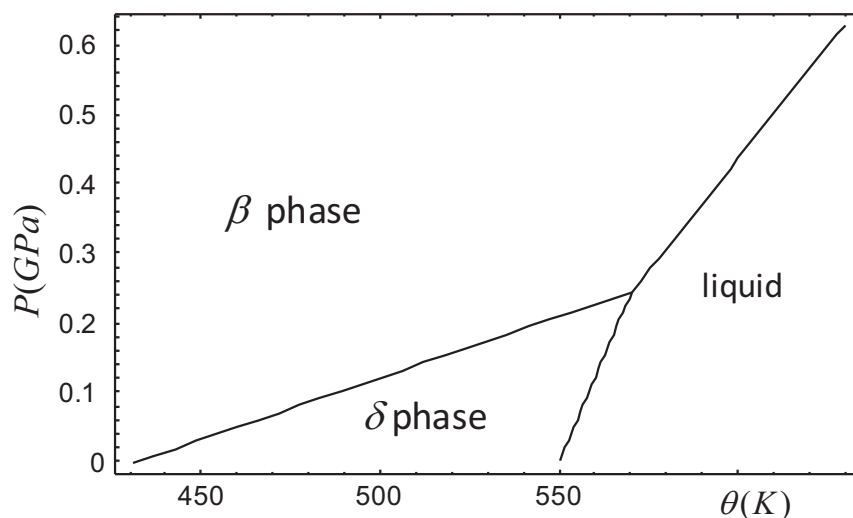


Figure 1: Calculated equilibrium pressure-temperature phase diagram

## NUCLEATION MECHANISM FOR THE RECONSTRUCTIVE SOLID-SOLID PHASE TRANSITION IN HMX VIA MELT MEDIATED NANO-CLUSTER TRANSFORMATION

### Experimental Observations

We recently observed a paradoxical experimental result:<sup>7-8</sup> the reconstructive  $\beta \rightarrow \delta$  PT in HMX starts at  $432.6^\circ\text{K}$ , just above the phase equilibrium temperature  $\theta_e = 432^\circ\text{K}$ . Even if  $\theta_e$  were several degrees lower (for example,

due to RDX inclusions), nucleation is still very close to  $\theta_e$  and all conclusions discussed below would remain valid.

The  $\beta \rightarrow \delta$  PT is accompanied by a large volumetric expansion,  $\varepsilon^t = 0.08$  (see Menikoff and Sewell).<sup>21</sup> Thus, the associated energy of internal stresses ( $g^e = 8.947 \text{ kJ/mol}$ , (see Levitas et al.<sup>11</sup>) is very large and, if not relaxed, should increase the PT temperature by  $g^e / \Delta s_{\beta \rightarrow \delta} = 400^\circ\text{K}$ . The additional nucleation barrier due to the interface energy makes even larger increase in the nucleation temperature possible. For example, for martensitic PT in steels (which requires deformation only and not reconstruction of the crystal lattice and for which the elastic energy can be easily relaxed through traditional slip and twinning mechanisms, in contrast to HMX),  $\varepsilon^t = 0.02$  but the PT onset temperature deviates from  $\theta_e$  by  $\sim 100^\circ\text{K}$ . Another example is the PT in KCl which (despite the volume increase of 11%) has relatively small pressure hysteresis of 0.4 GPa, i.e. the deviation of transformation pressure from the equilibrium pressure is 0.2 GPa. Using the pressure-temperature equilibrium line for  $\beta - \delta$  PT [Eq. (7)], 0.6°K of the deviation of the transformation temperature from the phase equilibrium temperature can be transformed to a pressure deviation of  $10^{-3}$  GPa, which is 200 times smaller than for KCl. No existing theory can explain nucleation so close to the equilibrium line.

The above result was obtained for PBX 9501, i.e. for HMX crystals bonded with a binder (Estane and nitroplasticizer). Our preliminary observations in Smilowitz et al.<sup>20</sup> led us to a hypothesis that  $\beta$  HMX dissolves in the molten nitroplasticizer, and at temperatures above  $\theta_e$  nucleates the  $\delta$  phase at the interface between the HMX and the liquid.

As we will show below, such a mechanism does completely remove the energy of elastic stresses. We also show that because of high interface energy any such homogeneous or heterogeneous nucleation is kinetically impossible close to the phase equilibrium temperature. We suggest below that the *liquid nitroplasticizer contains nanometer size clusters of  $\beta$  phase*, which may appear during dissolution of HMX in the liquid and the destruction of HMX surface asperities. The reconstructive  $\beta \rightarrow \delta$  PT in such a cluster is accompanied by a small (or even negative) change in interface energy and allows nucleation of the  $\delta$  phase near the phase equilibrium temperature. Using this mechanism, a thermally activated nucleation kinetics is derived.<sup>19</sup> We combine it in Section V with our recent results on the virtual melting growth mechanism<sup>11,14-16</sup> to develop a physically based kinetic model for the  $\beta \rightarrow \delta$  PT which is in very good correspondence with our experiments.

### **New Nucleation Mechanism and Kinetics**

We first show here that the surface nucleation mechanism discussed above<sup>20</sup> completely relaxes the large energy of internal stresses (8.947 kJ/mol (see

Levitas et al.<sup>11)</sup> that would be generated during direct solid-solid PT. Let nucleation occur in a closed liquid cavity with volume  $V_l$ ; then the elastic energy due to the volume change is equal to  $0.5^\circ\text{K } \varepsilon_0^2$ . Here  $\varepsilon_0 = \varepsilon' V_n/V_l$  is the volumetric strain in the liquid,  $V_n$  is the volume of the  $\delta$  phase nucleus and  $K$  is the bulk modulus of the liquid. Assuming conservatively the volume of the liquid nitroplasticizer near each HMX crystal  $V_l = 10^5 \cdot 10^5 \cdot 10^4 = 10^{14} \text{nm}^3$  and the volume of nucleus  $V_n = 10^3 \text{nm}^3$  (see our estimates below), we derive  $\varepsilon_0 = 10^{-11} \varepsilon' = 8 \cdot 10^{-13}$  which is negligible. Since, in reality, volume  $V_l$  is not closed, volumetric strain  $\varepsilon_0$  is even smaller.

### Impossibility of a classical homogeneous and heterogeneous nucleation

Despite the relaxation of internal stresses, the nucleation barrier due to the interface energy is still too large to allow such a nucleation mechanism close to the phase equilibrium temperature. The mean time for a thermally activated nucleation is described by the Arrhenius equation<sup>26-27</sup>

$$t_n = \tilde{t} \frac{h}{k\theta} \exp\left(\frac{E_n}{k\theta}\right) = \frac{\bar{t}}{\theta} \exp\left(\frac{E_n}{k\theta}\right), \quad (10)$$

where  $k = 1.381 \cdot 10^{-23} \text{J/K}$  and  $h = 6.626 \cdot 10^{-34} \text{Js}$  are Boltzmann's and Planck's constants,  $E_n$  is the activation energy for nucleation and  $\bar{t}$  and  $\tilde{t}$  are pre-exponential multipliers (determined below from the best fit to experimental data). The activation energy is equal to the energy of a critical nucleus. For a spherical nucleus, it is described by the well known equation:<sup>26</sup>

$$E_n = \frac{16\pi\Delta\gamma^3}{3\Delta G_{\beta \rightarrow \delta}^2}, \quad (11)$$

where  $\Delta\gamma$  is the change in surface energy. For precipitation of the  $\delta$  phase from the solution of HMX in liquid nitroplasticizer,  $\Delta G_{\beta \rightarrow \delta}$  has to take into account the thermodynamic properties of solution. They are unknown, so we will use the difference in the Gibbs potential of  $\beta$  and  $\delta$  phases, which as we will see does not change our conclusions. Substituting  $\Delta G_{\beta \rightarrow \delta}$  and all the above data in Eq. (11), one obtains for  $p = 0$

$$E_n = \frac{8.366 \cdot 10^{-10} \Delta\gamma^3}{(\theta - 432)^2}. \quad (12)$$

Nucleation can occur during the time of an experiment only if  $E_n = 40k$  to  $80k\theta$  (see Porter and Easterling<sup>26</sup>). Indeed, for  $E_n = 40$  to  $80k\theta$ ,  $\exp(E_n/k\theta) = 10^{17} - 10^{34}$ . For  $\bar{t}/\theta = 10^{-17} \text{s}$  (which has the meaning of the nucleation time for  $E_n = 0$ ), Eq. (10) results in nucleation time  $t_n = (1-10^{17})\text{s}$  that can be realized in experiments or in nature. On the other hand, for  $\gamma_{s-l} = 6 \cdot 10^{-2} \text{J/m}^2$  and  $\theta = 432.6^\circ\text{K}$ , we obtain from Eq. (10)  $t_n = 10^{36489442} \text{s}$ ; for  $\gamma_{s-l} = 10^{-2} \text{J/m}^2$  and  $\theta =$

438°K (which increases  $\Delta G_{\beta \rightarrow \delta}$  by a factor of 10), we still have  $t_n = 10^{1646} s$ , which is absolutely unrealistic for an actual nucleation.

Taking  $\theta = 432.6^\circ K$  and  $E_n = 80k\theta$ , we estimate from Eq. (12) the change in surface energy of  $\Delta\gamma < 6 \cdot 10^{-4} J/m^2$  that allows the nucleation. This number is extremely small in comparison with reality. For homogeneous nucleation of  $\delta$  crystals in the molten nitroplasticizer,  $\Delta\gamma$  is the interface energy between the solid  $\delta$  phase and liquid nitroplasticizer,  $\gamma_{\delta-l}$ . Usually, the solid-liquid interface energy is of the order of magnitude  $\gamma_{s-l} = 10^{-1} - 10^{-2} J/m^2$ . Consequently, homogeneous nucleation is impossible, like for most PTs. Assuming  $\gamma_{s-l} = 6 \cdot 10^{-2} J/m^2$ , then the activation energy for homogeneous nucleation is six orders of magnitude larger than allowable by the equation  $E_n = 80k\theta$ . Even for  $\gamma_{s-l} = 10^{-2} J/m^2$ , an eventual increase in the driving force for a PT by one order of magnitude, due to the temperature dependence in  $-\Delta G_{\beta \rightarrow \delta}$ , by an eventual chemical reaction, or by the thermodynamics of dissolution of HMX in the liquid phase, does not change our conclusion that the homogeneous nucleation is impossible.

For heterogeneous nucleation at the flat surface of the  $\beta$  phase one obtains<sup>26</sup>

$$E_n = \frac{8.366 \cdot 10^{-10} \gamma_{\delta-l}^3}{(\theta - 432)^2} S(\alpha); \quad S(\alpha) := \frac{(2 + \cos\alpha)(1 - \cos\alpha)^2}{4}. \quad (13)$$

Here the wetting angle  $\alpha$  is determined by the mechanical equilibrium of the components of surface tension along the flat interface,<sup>26</sup> namely  $\gamma_{\beta-l} = \gamma_{\beta-\delta} + \gamma_{\delta-l} \cos\alpha$  (i.e.  $\cos\alpha = (\gamma_{\beta-l} - \gamma_{\beta-\delta})/\gamma_{\delta-l}$ ), where  $\gamma_{\beta-l}$  is the energy of interfaces between the  $\beta$  phase and surrounding liquid and  $\gamma_{\beta-\delta}$  is the  $\beta$ - $\delta$  interface energy. A low-energy coherent interface between the  $\beta$  and  $\delta$  phases cannot be expected because it will cause a significant increase in elastic energy of internal stresses and create an additional thermodynamic barrier to nucleation. Usual estimates for an incoherent interface are  $\gamma_{\beta-\delta} \simeq 1 J/m^2 \simeq 10\gamma_{s-l}$  to  $100\gamma_{s-l}$ . Heterogeneous nucleation is favorable in comparison with the homogeneous one for  $\cos\alpha \simeq 1$ , i.e. for  $\gamma_{\beta-l} \gg \gamma_{\beta-\delta}$ . In fact, our case is the opposite, i.e.  $\gamma_{\beta-l} \ll \gamma_{\beta-\delta}$ . For such a situation, the mechanical equilibrium  $\gamma_{\beta-l} = \gamma_{\beta-\delta} + \gamma_{\beta-l} \cos\alpha$  is not satisfied and wetting is impossible. Thus, heterogeneous nucleation at the interface between liquid and  $\beta$  phase is kinetically even less favorable than homogeneous nucleation.

### Nucleation mechanism via cluster to cluster transformation

Let us consider the following mechanism of  $\beta \rightarrow \delta$  PT through a liquid nitroplasticizer. We assume that the *liquid medium contains nanometer size clusters of  $\beta$  phase* that may appear during destruction of HMX surface asperities and their suspension in the liquid. When such a cluster undergoes the reconstructive  $\beta \rightarrow \delta$  PT, then the activation energy for nucleation is determined by the same Eq. (11) [or Eq.(12)] but with different change in

surface energy,  $\Delta\gamma = \gamma_{\delta-l} - \gamma_{\beta-l}$ . Both  $\gamma_{\delta-l}$  and  $\gamma_{\beta-l}$  are large but are of the same order of magnitude. Then their difference,  $\gamma_{\delta-l} - \gamma_{\beta-l}$ , can be much smaller than each of them ( $\gamma_{\delta-l}$  or  $\gamma_{\beta-l}$ ), i.e. it can be as small as  $(4.7-5.9) \cdot 10^{-4} J/m^2$  required by the kinetic nucleation condition  $E_n = 40$  to  $80k\theta$  [26], or even smaller. Moreover, for one of the PTs,  $\beta \rightarrow \delta$  or  $\delta \rightarrow \beta$ , the change in interface energy  $\Delta\gamma$  is negative, because they differ by a sign only. This means that the barrier less nucleation of the  $\delta$  (or  $\beta$ ) phase may occur in the  $\beta$  (or  $\delta$ ) cluster. The radius of the critical cluster is determined by the well known equation<sup>26</sup>

$$r_c = \frac{2\Delta\gamma}{\Delta G_{\beta \rightarrow \delta}} = 1.4 \cdot 10^{-5} \frac{\Delta\gamma}{(\theta - 432)} \quad (14)$$

For  $\theta = 432.6$  and  $\Delta\gamma = 4.78 \cdot 10^{-4} J/m^2$  (the value that will be obtained below), we calculate the radius of  $r_c = 11nm$ ; a decrease in change of the interface energy  $\Delta\gamma$  or increase in the deviation from the phase equilibrium temperature,  $\theta - 432$ , reduces the cluster radius proportionally.

The region near the interface between the  $\beta$  phase and nitroplasticizer is the most probable place where a critical  $\delta$  phase cluster may nucleate. The nucleus can grow via dissolution of the surface of the  $\beta$  phase crystal, diffusion of molecules through nitroplasticizer toward the growing  $\delta$  crystal, and subsequent crystallization onto the surface of the stable  $\delta$  cluster. The observable macroscopic growth kinetics will only be determined by those nuclei from the entire population of supercritical nuclei (that are usually called operational nuclei) that are close enough to the interface with the  $\beta$  phase and have the smallest diffusion path. Some  $\delta$  crystals may touch the  $\beta$  crystal surface (in particular, due to gravitational and/or electrostatic forces) and form a new  $\beta - \delta$  interface. This interface initially contains a very thin layer of nitroplasticizer; when the interface area grows due to the  $\beta \rightarrow \delta$  PT, content of the nitroplasticizer in the interface is negligible. Thus, the suggested melt mediated cluster to cluster PT nucleation mechanism completely relaxes the elastic energy of internal stresses and reduces by orders of magnitude the change in interfacial energy. That is why it makes possible nucleation very close to the phase equilibrium temperature and it initiates the virtual melting mechanism of growth in the bulk by contact of  $\delta$  clusters with the  $\beta$  surface phase of larger crystals. This mechanism will be further elaborated and used below for the development a fully physical overall kinetic model for the  $\beta \rightarrow \delta$  PT.

Note that for slow heating ( $1^\circ K/hour$ ) of LX-04 explosive, consisting of 85% by weight of HMX and 15% of Viton A binder, PT in HMX starts at  $436^\circ K$ , which is close to  $433^\circ$  for PBX-9501 explosive, <sup>28</sup> while Viton A does not melt in the PT temperature range. We can speculate that Viton A partially decomposes or significantly softens producing hydrostatic or quasi-hydrostatic medium in which  $\beta$ -HMX clusters suspend and transform into  $\delta$  phase. However, more detailed study is required.

## GROWTH MECHANISM AND KINETICS FOR $\beta \leftrightarrow \delta$ PHASE TRANSFORMATION IN HMX VIA VIRTUAL MELTING

### Virtual Melting Growth Mechanism

During the solid-solid PT, the transformation strain may generate two types of internal elastic stresses:

- a) Due to the displacement continuity across a coherent interface. If the interface completely (or partially) loses its coherence, these stresses completely (or partially) relax.
- b) Due to a change in volume during the PT, the  $\delta$  phase is completely embedded inside the  $\beta$  phase. Even loss of interface coherence does not relax these stresses.

The energy of the internal stresses increases the PT temperature. However, since nucleation and growth of the  $\delta$  phase in PBX 9501 starts at the surface of the  $\beta$  crystal, the type b) of internal stresses can be neglected. They are important, however, for the PT in crystalline HMX without the binder where the PT starts inside the crystal at some nucleation sites.

We demonstrated earlier<sup>11,14,15</sup> that the energy of the internal stresses of type a) at the initially coherent  $\beta - \delta$  interface ( $g^e = 8.947 \text{ kJ/mol}$ ) is sufficient to make the energy of the stressed layer of the  $\delta$  phase equal to the energy of the melt. Thus, it melts approximately 120°K below the normal melting temperature of the  $\delta$  phase,  $\theta_{m,\delta} = 550^\circ\text{K}$ , i.e. around the  $\beta - \delta$  phase equilibrium temperature of  $\theta_e = 432^\circ\text{K}$  at ambient pressure during the  $\beta \rightarrow \delta$  PT. It is also sufficient to reduce the melting temperature of the  $\beta$  phase from 520°K to 400°K for the  $\beta$  phase during the  $\delta \rightarrow \delta$  PT. Melting of the thin layer is accompanied by a decrease in the interface energies, i.e. the melt nucleation is barrier less.<sup>11,14</sup> After melting, the elastic stresses completely relax and the interface completely loses its coherence. A stress-free melt is unstable with respect to stable  $\delta$  phase, and it solidifies into the  $\delta$  phase. The melt in each transforming material point exists during an extremely short time required for stress relaxation. We called it the virtual melt, because it represents a transitional activated state rather than a thermodynamically stable melt.

A volume decrease during solidification results in tensile stresses in the solidifying layer of the  $\delta$  phase. Since resistance to fracture during solidification is negligible, the elastic strains completely relax through nanocracking, vacancy, and void generation. Estimates in Levitas et al.<sup>14</sup> show that the volumetric strain due to cracking  $\varepsilon^c = -2\varepsilon_{\delta-m}^t/3 = 0.045$ , where  $\varepsilon_{\delta-m}^t = 0.067$  is the volumetric transformation strain for solidification. This is the upper bound for the porosity induced by this mechanism when external pressure is absent.

The characteristic size of the initial cavities is of few nanometer sizes. Since nanocracking occurs sequentially in the entire transforming volume, the size of the cracks and voids may grow by diffusion and coalescence, since the temperature is not too far from the melting temperature. The solidification explains the nanoporosity that was observed in experiments in various published works.<sup>7,8,23,6,29</sup> Without the virtual melting, compressive stresses caused by the expansion of the  $\delta$  phase could not lead to nanocracking. Note that in Hsu et al.,<sup>29</sup> fraction of open and closed pores in LX-10 sample after heating to 190°C increased by 9.71% and 2.46%, respectively. We, however, cannot compare these data directly with our estimates because it is not clear which part of porosity is caused by PT and is concentrated in HMX.

The nanoporosity during the solidification is generated when stresses are near zero, and that is why it does not change the thermodynamics and kinetics of the  $\beta \rightarrow \delta$  PT; the virtual melting eliminates the whole thermomechanical memory of preceding cycles of the  $\beta \leftrightarrow \delta$  PT.<sup>11,14,15</sup> These results explain the paradoxical independence of the thermodynamics and kinetics for the first and the second direct-reverse transformation cycles that was observed in experiments by Henson et al.<sup>7</sup> and Smilowitz et al.<sup>8</sup> Under high external pressure, we assume that porosity will be closed immediately after its appearance because the yield stress is close to zero. Thus, we neglect the damage during the  $\beta \rightarrow \delta$  PT via virtual melting. Also, the athermal interface friction  $K_{at}$  disappears for the virtual melting growth mechanism because the melt as a hydrostatic medium does not interact with the long range stress field of the crystal lattice defects.<sup>11,14,15</sup> This explains why the transformation can progress under a surprisingly small thermodynamic driving force. For the other PTs in the HMX system, like  $\alpha \leftrightarrow \delta$  and  $\alpha \leftrightarrow \beta$ , the change in volume is approximately two times smaller and cannot cause melting. This unrelaxed elastic energy and athermal interface friction explains the relatively large temperature hysteresis observed in these systems. In particular,  $\beta \rightarrow \alpha$  PT does not occur at all and  $\beta$  phase transforms directly to  $\delta$  HMX.<sup>2</sup> In total, sixteen theoretical predictions are in qualitative and quantitative correspondence with experiments performed on the PTs in the HMX energetic crystal.

### Growth Kinetics

The velocity of the  $\beta - \delta$  phase interface can be described by the thermally activated kinetics<sup>14</sup> utilizing the virtual melting mechanism:

$$v = \bar{v}_0 \left( \exp\left(-\frac{g_{\beta \rightarrow m}}{R\theta}\right) - \exp\left(-\frac{g_{\delta \rightarrow m}}{R\theta}\right) \right) = \bar{v}_0 \exp\left(-\frac{g_{\delta \rightarrow m}}{R\theta}\right) \left( \exp\left(-\frac{g_{\beta \rightarrow \delta}}{R\theta}\right) - 1 \right), \quad (15)$$

where  $\bar{v}_0$  is the pre-exponential factor. Since

$$\begin{aligned} \bar{v}_0 \exp\left(-\frac{g_{\delta \rightarrow m}}{R\theta}\right) &= \bar{v}_0 \exp\left(-\frac{\Delta h_{\delta \rightarrow m} - \theta \Delta s_{\delta \rightarrow m} + p \Delta v_{\delta \rightarrow m}}{R\theta}\right) = \\ \bar{v}_0 \exp\left(\frac{\Delta s_{\delta \rightarrow m}}{R}\right) \exp\left(-\frac{\Delta h_{\delta \rightarrow m} + p \Delta v_{\delta \rightarrow m}}{R\theta}\right) &= v_0 \exp\left(-\frac{\Delta h_{\delta \rightarrow m} + p \Delta v_{\delta \rightarrow m}}{R\theta}\right), \end{aligned}$$

where  $v_0 = \bar{v}_0 \exp\left(-\frac{\Delta s_{\delta \rightarrow m}}{R}\right)$ , then

$$v = v_0 \exp\left(-\frac{\Delta h + p \Delta v_{\delta \rightarrow m}}{R\theta}\right) \left[ \exp\left(-\frac{\Delta g_{\beta \rightarrow \delta}}{R\theta}\right) - 1 \right], \quad (16)$$

where  $v_0$  was found in Levitas et al.<sup>11,15</sup> to be  $10^{10} \mu\text{m/s} = 10^4 \text{m/s}$ . We put  $K_{at} = 0$  (in contrast to all known solid-solid PTs), because liquid, as the hydrostatic medium, does not interact with the stress field of crystal defects, consequently, the athermal resistance to interface propagation is absent. The term in square parenthesis is a function of the driving force for  $\beta \rightarrow \delta$  PT, which is equal to zero for thermodynamic equilibrium and greater (smaller) than zero in the region of stability of the  $\delta$  ( $\beta$ ) phase; Eq. (16) is valid for both  $\beta \rightarrow \delta$  (for  $v > 0$ ) and  $\delta \rightarrow \beta$  (for  $v < 0$ ) PT. The temperature dependence of the rate constant is determined by the heat of fusion  $h_{\delta \rightarrow m}$  and transformation work of fusion  $p \Delta v_{\delta \rightarrow m}$ . Predictions of Eq. (16) are in a good agreement with various experiments under ambient pressure (see Levitas, et al.<sup>11,15,16</sup>) including experiments in Wernhoff et al.<sup>10</sup> The time derivative of the volume fraction of the  $\delta$  phase due to interface motion,  $\dot{c}$  can be determined by the approximate equation

$$\dot{c} = \int_{\Sigma} v d \Sigma / V = v_{av} \Sigma / V, \quad (17)$$

where  $V$  is the volume of the crystal,  $\Sigma$  is the total area of the  $\beta$ - $\delta$  interface and  $v_{av}$  is the averaged interface velocity over the area  $\Sigma$ . The total area of interfaces is a function of the propagation geometry. For example, in the case where the interface propagates from one end to another of the prismatic specimen and it is perpendicular to the axis of the specimen, the area is constant during the entire propagation process and has jumps from zero to  $\Sigma$  and from  $\Sigma$  to zero at the beginning and the end of PT, respectively. For the case with numerous interfaces of stochastic geometry, the approximation  $\Sigma \sim c(1-c)$  can be used. The last equation at least satisfies two limiting cases of zero area at the beginning and end of PT. If we consider a group of HMX crystals and in each of them there is a single interface, but the interface geometry in each

crystal is different, then the interface area  $\Sigma$  averaged over the group of crystals is similar to that for a single crystal with a stochastic interface geometry, i.e.  $\Sigma \sim c(1-c)$ .

Assuming that  $v_{av}$  can be determined by Eq. (16), one obtains

$$\dot{c}_g = B v c(1-c) = \bar{c}_g c(1-c) \exp\left(-\frac{\Delta h_{\delta \rightarrow m} + p \Delta v_{\delta-m}}{R\theta}\right) \times \left[\exp\left(-\frac{\Delta g_{\beta \rightarrow \delta}}{R\theta}\right) - 1\right] \quad (18)$$

Here,  $B$  and  $\bar{c}_g$  are the parameters that will be found from experiments. According to transition state theory,<sup>27</sup> we assume (similar to nucleation)  $\bar{c}_g = Z \frac{k\theta}{h}$ , where  $Z$  is the parameter that will be determined from the best fit to experiments.

### OVERALL KINETICS OF $\beta \leftrightarrow \delta$ PHASE TRANSFORMATION IN HMX

The overall nucleation and growth kinetics is described by the kinetic growth, Eq. (18) supplemented by the nucleation-motivated initial condition:

$$\dot{c} = bc(1-c); \quad c(t_0) = c_0. \quad (19)$$

$$b := Z \frac{k\theta}{h} \exp\left(-\frac{\Delta h_{\delta \rightarrow m} + p \Delta v_{\delta-m}}{R\theta}\right) \left[\exp\left(-\frac{\Delta g_{\beta \rightarrow \delta}}{R\theta}\right) - 1\right]. \quad (20)$$

We need to distinguish between a critical nucleus, i.e. a nucleus that corresponds to a maximum of Gibbs energy and has equal probability to grow or disappear, and an operational nucleus, i.e. a nucleus which cannot disappear and for which the volume fraction  $c_0$  that is reached at time  $t_0$  can be used as an initial condition in the overall macroscopic kinetic equation. There are a number of unknown parameters, like the diffusion coefficient and path, rate of dissolution and crystallization, which do not allow us to describe in detail the diffusional growth of a critical nucleus to the operational one. That is why we assume in the first approximation that  $t_0$  is proportional to  $t_n$ , i.e. from Eq. (10)

$$t_0 = \frac{\bar{t}_0}{\theta} \exp\left(\frac{E_n}{k\theta}\right) = \frac{\bar{t}_0}{\theta} \exp\left(\frac{16\pi\Delta\gamma^3}{3\Delta G_{\beta \rightarrow \delta}^2 k\theta}\right), \quad (21)$$

where  $\bar{t}_0$  is the pre-exponential factor. We also assume that the volume fraction of an operational nucleus  $c_0$  is a constant. For ambient pressure, Eq. (21) simplifies to:

$$t_0 = \frac{\bar{t}_0}{\theta} \exp\left(\frac{6.058 \cdot 10^{13} \Delta\gamma^3}{(\theta - 432)^2 \theta}\right) \quad (22)$$

The analytical solution to Eq. (19) under constant temperature and pressure is as follows:

$$c = \frac{c_0}{c_0 + (1 - c_0)\exp(-b(t - t_0))}. \quad (23)$$

For  $c = 0.5$ , one can find the time to half conversion which was used by Henson,<sup>7</sup> Smilowitz,<sup>8</sup> Burnham,<sup>9</sup> and other authors to compare with experiments. This leads to

$$t_{0.5} = t_0 + \frac{\ln\left(\frac{1}{c_0} - 1\right)}{b}. \quad (24)$$

More generally, the time to reach the volume fraction  $f$  can be found from the condition  $c = f$ :

$$t_f = t_0 + \frac{\ln\left(\frac{(1 - c_0)f}{c_0(1 - f)}\right)}{b}. \quad (25)$$

Thus, the time to reach any volume fraction  $f$  consists of the time for appearance of an operational nucleus  $t_0$  and time for its growth.

### Parameter Identification and Comparison with Experiments

Substituting into Eq. (24) for the time to half conversion, Eq. (22) for nucleation time  $t_0$  and Eq. (20) for the coefficient  $b$ , we obtain that  $t_{0.5}$  depends on three material parameters:  $\Delta\gamma$ ,  $\bar{t}_0$ , and  $\bar{Q} = \ln\left(\frac{1}{c_0} - 1\right)/Z$ . In Fig. 2, a good agreement between the prediction of Eq. (24) and the experimental data for  $t_{0.5}$  for  $\beta \rightarrow \delta$  transformation<sup>7,8</sup> was obtained. Parameters  $\Delta\gamma = 4.78 \cdot 10^{-4} \text{ J/m}^2$ ,  $\bar{t}_0 = 4.5 \cdot 10^{-4} \text{ sK}$ , and  $\bar{Q} = 5.822 \cdot 10^{12}$  are determined from the best fit to experiments for the time to half conversion. Even extrapolation of our equation for  $\theta = 550^\circ\text{K}$ , where our nucleation and growth mechanisms may not be operative, gives good agreement (Fig. 2) with a laser heating experiment.<sup>30</sup> Parameters  $Z$  and  $c_0$  can be varied in order to achieve the best correspondence between predicted and experimental shape of the  $c(t)$  curves. However, this degree of freedom is not necessary. We did not change our virtual melting based growth model<sup>16</sup> and retain the value of the parameter  $Z = 7 \cdot 10^{-13}$ ; that gives us  $c_0 = 0.016$  for the concentration of the operational nucleus.

Figure 3 exhibits a very good correspondence between kinetic curves predicted by Eq. (23) and the experiment. Note that extrapolation to a wider range of parameters (pressure and temperature) is much more reliable for the present physical model than for the phenomenological model in Levitas et al.<sup>16</sup>

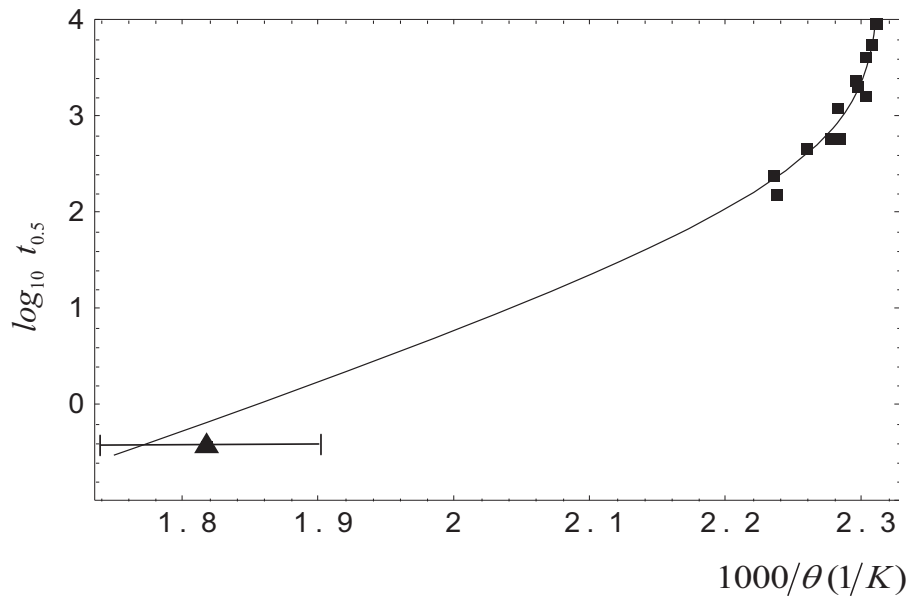


Figure 2: A comparison of the predictions of Eq. (24) (solid line) with experimental data.<sup>17,19</sup> The logarithm of the time to half conversion versus  $1000/\theta(K)$  for  $\beta \rightarrow \delta$  PT in the HMX based plastic bonded explosive PBX 9501. Squares are data from measurements made by second harmonic generation,<sup>7-8</sup> the triangle is the conversion half time measured during laser heating.<sup>30</sup>

Note that for diffusional PTs  $\bar{t}_0/\theta$  in Eq. (22) has to be presented in the form  $\hat{t}_{exp}(Q_{sd}/k\theta)$ , where  $Q_{sd}$  is the activation energy of self-diffusion<sup>26</sup> [the same is valid for Eq. (10)]. Also,  $\hat{t}$  should be proportional to the averaged area of HMX crystal, where nucleation occurs. However, this does not change our model because of the much stronger temperature dependence of  $t_0$  due to  $E_n$ . In the narrow temperature range where  $t_0$  is greater than or comparable with propagation time, both equations give very close results. At higher temperatures,  $t_0$  is negligible in Eq. (24). That is also why we are unable to determine  $Q_{sd}$  with reasonable accuracy.

### Nucleation under Variable Temperature and Pressure

If temperature and pressure are variable, the nucleation time  $t_0$  has to be evaluated starting with the instant when the PT criterion is met. Since we will consider only relatively slow loading and changes in temperature and pressure that are small during the nucleation time, we will use Eq. (21) substituting in it the values of temperature and pressure at time  $t_0$ , i.e.  $\theta(t_0)$  and  $p(t_0, c_0)$ :

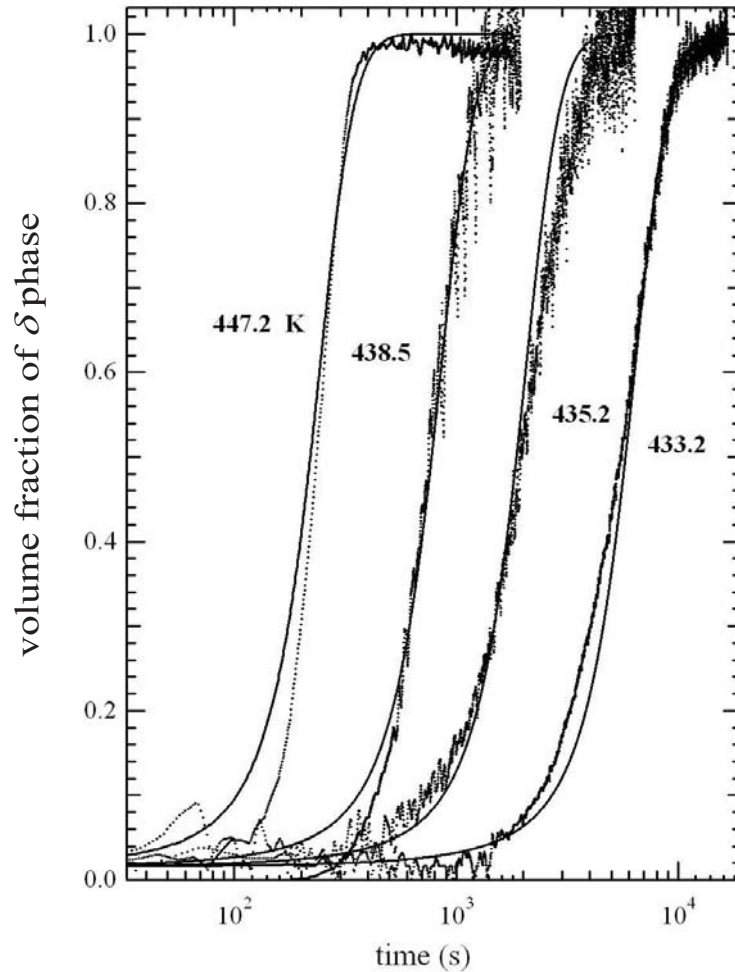


Figure 3: A comparison between prediction of Eq. (23) (solid curves) with experimental data for  $\beta \rightarrow \delta$  PT in the HMX based plastic bonded explosive PBX 9501<sup>7,8</sup> under isothermal conditions.<sup>17,19</sup> The volume fraction of the  $\delta$  phase  $c$  is equal to square root of the measured second harmonic generation intensity from the HMX  $\delta$  phase. The zero of time is the point at which the heated sample reached the labeled isothermal temperature.

$$t_0 = \frac{\bar{t}_0}{\theta(t_0)} \exp\left(\frac{16\pi M^2 \Delta\gamma^3}{3(\Delta S_{\beta \rightarrow \delta}(\theta(t_0)) - \theta_e) - p(t_0, c_0) \Delta v_{\beta - \delta})^2 \rho_h^2 k \theta(t_0)}\right). \quad (26)$$

This nonlinear algebraic equation has to be solved numerically for  $t_0$ . Note that the appearance of operational nuclei with  $c_0 = 0.016$  causes an instantaneous pressure change. This has to be defined from the solution of the mechanical problem and taken into account in  $p(t_0, c_0)$  in Eq. (26).

In the problem considered in Levitas et al.<sup>18</sup> (heating a PBX formulation in a rigid cylinder) a constant temperature rate,  $h_r$ , is prescribed and pressure  $p(\theta)$  is determined as a function of  $\theta$  from the solution of the mechanical problem. First, the mechanical problem without PT is solved, and temperature  $\theta_i$  at which PT criterion is met is determined from the nonlinear equation  $\Delta s_{\beta \rightarrow \delta}(\theta_i - \theta_e) = p(\theta_i)\Delta v_{\beta \rightarrow \delta}$ . Since  $\theta = \theta_i + h_r t$ , we can express time in terms of  $\theta$ , i.e.  $t = (\theta - \theta_i)/h_r$  and use temperature as an independent variable. Then, introducing the constant  $c = c_0$  in the mechanical problem, and expressing the solution  $p(t, c_0)$  in terms of temperature, we can determine the nucleation temperature,  $\theta_0$ , from the equation

$$\frac{\theta_0 - \theta_i}{h_r} = \frac{\bar{t}_0}{\theta_0} \exp\left(\frac{16\pi M^2 \Delta \gamma^3}{3(\Delta s_{\beta \rightarrow \delta}(\theta_0 - \theta_e) - p(\theta_0, c_0)\Delta v_{\beta \rightarrow \delta})^2 \rho_h^2 k \theta_0}\right). \quad (27)$$

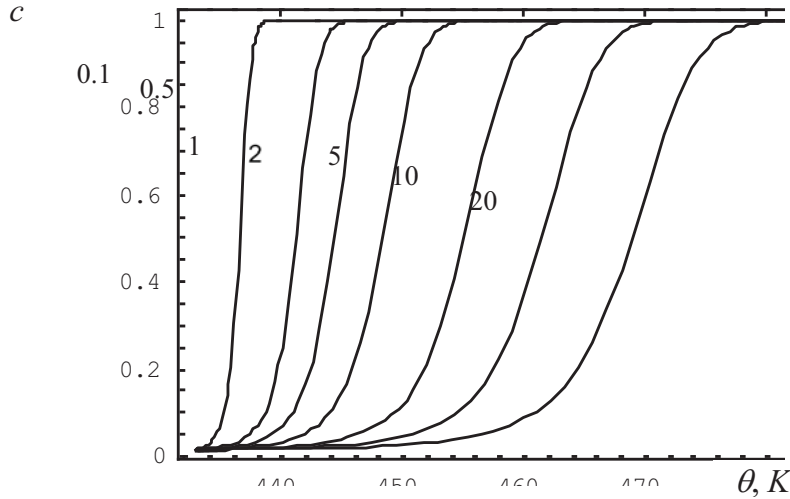


Figure 4: Evolution of the volume fraction of the  $\delta$  phase based on solution of Eqs.(19), (20) and (27) under zero pressure and various heating rates (shown in  $K/min$  near the curves)<sup>17</sup>.

Kinetic curves for the  $\beta \rightarrow \delta$  PT for zero pressure and various heating rates are shown in Fig. 4. Note that the nucleation temperature varies in a very narrow range from  $432.86^\circ K$  for  $h_r = 0.1^\circ K/min$  to  $433.0^\circ K$  for  $h_r = 20^\circ K/min$ . Despite the fact that the nucleation time at isothermal conditions of  $432.86^\circ K$  is 566 s and at  $433.0^\circ K$  is 3 s, multiplication of each of these times by the corresponding heating rate gives approximately the same temperature increment of  $1^\circ K$ . Thus, the main difference in the kinetic curves for different heating rates is due to the temperature dependence of the growth stage.

## CONCLUSION

The main results of this paper are:

- a) Elaborating a new nucleation mechanism for the  $\beta \rightarrow \delta$  PT in the energetic crystal HMX in the presence of a liquid binder and
- b) Development of the fully physical model for the overall kinetics of the  $\beta \leftrightarrow \delta$  PTs based on the above nucleation mechanism and the growth mechanism via the virtual melting.

Note that the knowledge of the suggested nucleation mechanism can be used to activate similar mechanisms for other PTs, especially with large volumetric strain and interface energy. This will allow a reduction of the PT pressure and temperature by substituting a direct solid-solid PT by a cluster-cluster PT in a proper liquid medium. It will also allow the discovery of new phases previously hidden due to large volumetric strain and interface energy, which cannot appear by a direct solid-solid PT. For example,  $\alpha$  HMX is stable at  $382.4 < \theta < 430^\circ\text{K}$ ; however,  $\beta$  HMX does not transform to  $\alpha$  in this temperature range; it transforms to  $\delta$  at  $\theta > 432^\circ\text{K}$ . In the presence of various solvents,  $\alpha$  HMX appears at  $382.4 < \theta < 430^\circ\text{K}$  (see Cady and Smith<sup>2</sup>). Furthermore, by a proper choice of solvent, one can nucleate and grow the desired metastable phase if the change of interface energy during cluster to cluster PT for this phase is significantly smaller than for the stable phase.

On the other hand, in the HMX crystals without a binder, nucleation occurs at the specific nucleating defects, which may be inclusions of the solvent used in HMX synthesis<sup>20</sup> or some stress concentrators. Nucleation temperature varies in a wide range from crystal to crystal because of different potencies of nucleation sites. For example, in Burnham et al.<sup>9</sup> the  $\beta \rightarrow \delta$  PT was not observed below  $448^\circ\text{K}$ . The case without the nitroplasticizer is not relevant for the current paper. However, it is relevant for the case when the nitroplasticizer disappears before the nucleation of the  $\delta$  phase.

The virtual melting transformation mechanism is also expected to be the main mechanism of pressure-induced crystal - crystal and crystal - amorphous PTs for a broad class of materials.<sup>31</sup> They occur in materials with the specific pressure - temperature phase diagram when the melting temperature of one of the phases reduces with growing pressure. This mechanism is expected in amorphization of ice,  $\alpha$ -quartz, coesite, jadeite, polymet, *Ge* and *Si*, BN and graphite.

Numerical analysis of the heating of PBX 9501 inside of a rigid cylinder based on the developed model is presented in Levitas et al.<sup>17-18</sup> The effect of the heating rate, initial porosity and pre-straining, and gas leaking rule on the

kinetics of the  $\beta \leftrightarrow \delta$  PT, HMX and binder decomposition and pressure build up is analyzed numerically.

## ACKNOWLEDGMENTS

Valery Levitas acknowledges the LANL contracts (13720-001-05-AH and 31553-002-06) and NSF grants (CMS-02011108 and CMS-0555909); Laura Smilowitz, Bryan Henson and Blaine Asay acknowledge the support of the Laboratory Research and Development and H.E. Science Programs at Los Alamos National Laboratory.

## REFERENCES

- <sup>1</sup>Asay, B.W., Parker, G., Dickson, P., Henson, B., and Smilowitz, L. (2004) On the Difference in Impact Sensitivity of Beta and Delta HMX, *J. Energetic Materials* **22**:223–35.
- <sup>2</sup>Cady, H.H. and Smith, L.C. (1962) Studies on the Polymorphs of the HMX, *LANL Report*, LAMS-2652.
- <sup>3</sup>Teetsov, A.S. and McCrone, W.C. (1965) Microscopical Study of Polymorph Stability Diagrams, *Microsc. Cryst. Front* **15**:13–29.
- <sup>4</sup>Karpowicz, R.J. and Brill, T.B. (1982) The Beta-Delta Transformation of HMX: Its Thermal Analysis and Relationship to Propellants, *AIAA J.* **20**:1586–90.
- <sup>5</sup>Boggs, T.L. (1984) The Thermal Behavior of Cyclotrimethylenetrinitramine (RDX) and Cyclotetramethylenetetranitramine (HMX), *Fundamentals of Solid Propellant Combustion*, K.K. Kuo and M. Summerfield, (eds.), AIAA Progress Series, Vol. 90, Chapter 3, 121–75.
- <sup>6</sup>Cady, H.H. (1986) Sensitivity and Handling Hazards of Delta-HMX Obtained by Heating PBX 9404, *Analyses of Propellants and Explosives, 17th International Annual Conference of ICT; Karlsruhe, FRG*, **17**:1–17.12.
- <sup>7</sup>Henson, B.F., Smilowitz, L.B., Asay, B.W., and Dickson, P.M. (2002) The Beta-Delta Phase Transition in the Energetic Nitramine Octahydro-1,3,5,7-Tetranitro-1,3,5,7-Tetrazocine: Thermodynamics, *J. Chemical Physics* **117**:3780–8.
- <sup>8</sup>Smilowitz, L.B., Henson, B.F., Asay, B.W., and Dickson, P.M. (2002) The Beta-Delta Phase Transition in the Energetic Nitramine Octahydro-1,3,5,7-Tetranitro-1,3,5,7-Tetrazocine: Kinetics, *J. Chemical Physics* **117**:3789–98.
- <sup>9</sup>Burnham, A.K., Weese, R.K., and Weeks, B.L. (2004) A Distributed Activation Energy Model of Thermodynamically Inhibited Nucleation and Growth Reaction and Its Application to the Beta-Delta Phase Transition of HMX, *J. Phys. Chem.* **B108**:19432–41.

- <sup>10</sup>Wemhoff, A.P., Burnham, A.K., and Nichols, A.L. (2007) Application of Global Kinetic Models to HMX Beta-Delta Transition and Cookoff Processes, *J. Phys. Chem. A* **111**:1575–84.
- <sup>11</sup>Levitas, V.I., Henson, B.F., Smilowitz, L.B., and Asay, B.W. (2006) Solid-Solid Phase Transformation via Internal Stress-Induced Virtual Melting, Significantly Below the Melting Temperature: Application to HMX Energetic Crystal, *J. Physical Chemistry B* **110**:10105–19.
- <sup>12</sup>Gump, J.C. and Peiris, S.M. (2005) Isothermal Equations of State of Beta Octahydro-1,3,5,7-Tetranitro-1,3,5,7-Tetrazocine at High Temperatures, *J. Appl. Phys.* **97**:05351.
- <sup>13</sup>Yoo, C.-H. and Cynn, H. (1999) Equation of State, Phase Transition, Decomposition of B-HMX Octahydro-1,3,5,7-Tetranitro-1,3,5,7-Tetrazocine at High Pressures, *J. Chem. Phys.* **111**:10229–35.
- <sup>14</sup>Levitas, V.I., Henson, B.F., Smilowitz, L.B., and Asay, B.W. (2004) Solid-Solid Phase Transformation via Virtual Melt, Significantly Below the Melting Temperature, *Phys. Rev. Lett.* **92**:235702.
- <sup>15</sup>Levitas, V.I., Henson, B.F., Smilowitz, L.B., Henson, B.F., and Asay, B.W. (2006) Solid-Solid Phase Transformation via Internal Stress-Induced Virtual Melting: Additional Confirmations, *Appl. Phys. Lett.* **87**:191907.
- <sup>16</sup>Levitas, V.I., Henson, B.F., Smilowitz, L.B., Henson, B.F., and Asay, B.W. (2006) Interfacial and Volumetric Kinetics of the Beta-Delta Phase Transition in the Energetic Nitramine Octahydro-1,3,5,7-Tetranitro-1,3,5,7-Tetrazocine Based on the Virtual Melting Mechanism, *J. Chem. Phys.* **124**:026101.
- <sup>17</sup> Levitas, V.I., Henson, B.F., Smilowitz, L.B., Zerkle, D.K., and Asay, B.W. (2007) Coupled Phase Transformation, Chemical Decomposition, and Deformation in Plastic-Bonded Explosive: Models, *J. Appl. Physics* **102**:113502.
- <sup>18</sup> Levitas, V.I., Henson, B.F., Smilowitz, L.B., Zerkle, D.K., and Asay, B.W. (2007) Coupled Phase Transformation, Chemical Decomposition, and Deformation in Plastic-Bonded Explosive: Simulations, *J. Appl. Physics* **102**:113520.
- <sup>19</sup>Levitas, V.I., Smilowitz, L.B., Henson, B.F., and Asay, B.W. (2006) Nucleation Mechanism for Reconstructive Solid-Solid Phase Transitions via Melt Mediated Nano-Cluster Transformation, *Applied Physics Letters* **89**:231930.
- <sup>20</sup>Smilowitz, L.B., Henson, B.F., Greenfield, M., Sas, A., Asay, B.W., and Dickson, P.M. (2004) On the Nucleation Mechanism of the Beta-Delta Phase Transition in the Energetic Nitramine Octahydro-1,3,5,7-Tetranitro-1,3,5,7-Tetrazocine, *J. Chemical Physics* **121**:5550–2.
- <sup>21</sup>Menikoff, R. and Sewell, T.D. (2002) Constituent Properties of HMX Needed for Mesoscale Simulations, *Combustion Theory and Modelling* **6**:103–25.

- <sup>22</sup>Sewell, T.D., Menikoff, R., Bedrov, D., and Smith, G.D. (2003) A Molecular Dynamics Simulation Study of Elastic Properties of HMX, *J. Chemical Physics* **119**:7417–26.
- <sup>23</sup>Weese, R.K. and Burnham, A.K. (2005) Coefficient of Thermal Expansion of the Beta and Delta Polymorphs of HMX, *Propellants, Explosives, Pyrotechnics* **30**:344–50.
- <sup>24</sup>Herrmann, M., Engel, W., and Eisenreich, N. (1992) Thermal Expansion, Transitions, Sensitivities and Burning Rates of HMX, *Propellants, Explosives, Pyrotechnics* **17**:190–95.
- <sup>25</sup>Lyman, J.L., Liao, Y.C., and Brand, H.V. (2002) Thermochemical Functions for Gas-Phase, 1,3,5,7-Tetranitro-1,3,5,7-Tetraazacyclooctane (HMX), Its Condensed Phases, and Its Larger Reaction Products, *Combustion and Flame* **130**:185–203.
- <sup>26</sup>Porter, D.A. and Easterling, K.E. (1989) *Phase Transformations in Metals and Alloys*, Van Nostrand Reinhold (International), London.
- <sup>27</sup>Hammes, G.G. (1978) *Principles of Chemical Kinetics*, Academic, New York, NY.
- <sup>28</sup>Wardell, J.F. and Maienschein, J.L. (2002) The Scaled Thermal Explosion Experiment, *Proceedings of 12th International Symposium on Detonation*, Office of Naval Research, San Diego, CA.
- <sup>29</sup>Hsu, P.C., Dehaven, M., McClelland, M. Traver, C., Chidester S., and Maienschein, J., (2006) Characterization of Damaged Materials, *Proceedings of 13th International Symposium on Detonation*, Office of Naval Research, Norfolk, VA.
- <sup>30</sup>Henson, B.F., Asay, B.W., Sander, R.K., Son, S.F., Robinson, J.M., and Dickson, P.M. (1999) Dynamic Measurement of the HMX Beta-Delta Phase Transition by Second Harmonic Generation, *Phys. Rev. Letters* **82**:1213–6.
- <sup>31</sup>Levitas, V.I. (2005) Crystal-Amorphous and Crystal-Crystal Phase Transformations via Virtual Melting, *Phys. Review Letters* **95**:075701.